Air-sea CO2 fluxes above the stratified oxygen minimum zone in the coastal region off Mexico

A. C. Franco-Novela, J. M. Hernández-Ayón, E. Beier, V. Garçon, H. Maske, A. Paulmier, J. Färber-Lorda, R. Castro-Valdez, R. Sosa-Avalos

AGU PUBLICATIONS

JGR

Journal of Geophysical Research: Oceans

RESEARCH ARTICLE

10.1002/2013JC009337

Key Points:
- Weak air-sea CO_2 fluxes were determined above a highly stratified coastal region
- El Niño masked seasonal variability while La Niña did not
- Positive fluxes to the atmosphere can be observed during cyclonic eddies

Correspondence to:
J. M. Hernández-Ayón,
jmartin@uabc.edu.mx

Citation:
Franco, A. C., J. M. Hernández-Ayón, E. Beier, V. Garçon, H. Maske, A. Paulmier, J. Färber-Lorda, R. Castro, and R. Sosa-Ávalos (2014), Air-sea CO_2 fluxes above the stratified oxygen minimum zone in the coastal region off Mexico, *J. Geophys. Res. Oceans*, *119*, 2923–2937, doi:10.1002/2013JC009337.

Received 6 AUG 2013
Accepted 19 APR 2014
Accepted article online 23 APR 2014
Published online 14 MAY 2014

Air-sea CO_2 fluxes above the stratified oxygen minimum zone in the coastal region off Mexico

Ana C. Franco[1], J. Martín Hernández-Ayón[2], Emilio Beier[3], Veronique Garçon[4], Helmut Maske[5], Aurelien Paulmier[4], Jaime Färber-Lorda[5], Rubén Castro[1], and Ramón Sosa-Ávalos[6]

[1]Facultad de Ciencias Marinas, Universidad Autónoma de Baja California, Baja California, Mexico, [2]Instituto de Investigaciones Oceanológicas, Universidad Autónoma de Baja California, Baja California, Mexico, [3]Centro de Investigación Científica y de Educación Superior de Ensenada, Unidad La Paz, Baja California, Mexico, [4]LEGOS, CNRS/IRD/UPS/CNES UMR 5566, Toulouse, France, [5]Centro de Investigación Científica y Educación Superior de Ensenada, Baja California, Mexico, [6]Facultad de Ciencias Marinas, Universidad de Colima, Manzanillo, Mexico

Abstract Oxygen minimum zones (OMZs) are important sources of CO_2 to the atmosphere when physical forces bring subsurface water with high dissolved inorganic carbon (DIC) to the surface. This study examines, for the first time, the influence of the OMZ of the coastal North Eastern Tropical Pacific off Mexico on surface CO_2 fluxes. We use variations in the oxycline depth and subsurface water masses to discern physical oceanographic influences. During two cruises, in November 2009 and August 2010, DIC and total alkalinity (TA) measurements were used to estimate pCO_2 and air-sea CO_2 fluxes. At the OMZ layer, Subtropical Subsurface Water (StSsW) was found to have high pCO_2 values (1290 $\pm$ 70 μatm). Due to strong vertical stratification, however, the relationship between ΔpCO_2 at the air-sea interface and the oxycline/StSsW upper limit depth was weak. During November, the region was a weak source of CO_2 to the atmosphere (up to 2.5 mmol C m^{-2} d^{-1}), while during August a range of values were observed between -4.4 and 3.3 mmol C m^{-2} d^{-1}). Strong stratification ($>$1200 J m^{-3}) prevented subsurface mixing of water from the OMZ to the upper layer; particularly in November 2009 which was during an El Niño event. Results suggest that advection of surface water masses, reinforced by strong vertical stratification, controlled surface pCO_2, and air-sea CO_2 fluxes.

1. Introduction

Shallow and extensive oxygen minimum zones (OMZs) are known to be important sources of CO_2 and other greenhouse gases to the atmosphere [*Paulmier et al*., 2008; *Friederich et al*., 2008]. OMZ layers occur at intermediate depths (100–800 m) where oxygen is consumed and dissolved inorganic carbon (DIC) is produced due to remineralization of sinking organic matter from the surface layer. Consequently, OMZs have also been called carbon maximum zones (CMZ) [*Paulmier et al*., 2011]. OMZ formation and maintenance is favored by strong vertical stratification and sluggish ventilation. Previous studies on OMZs have related the magnitude and direction of the air-sea CO_2 fluxes to physical mechanisms, which connected the surface and subsurface layers [*Paulmier et al*., 2008]; specifically, vertical mixing and upwelling events. For example, *Friederich et al*. [2008] found that the OMZ off Peru (5°S–20°S), a region of intense upwelling, acts as a source of CO_2 to the atmosphere year round (providing up to 5.7 mol m^{-2} y^{-1}). The OMZ in the Arabian Sea (10°N–18°N) also acts as a source of CO_2 to the atmosphere ($\Delta pCO_2 \sim 450$ μatm) when subsurface water rises to the surface as a result of intense vertical mixing during the monsoon season [*Körtsinger et al*., 1997].

The most extensive OMZ is found in the North Eastern Tropical Pacific (hereafter NETP). Here the concentration of oxygen is less than 45 μmol kg^{-1} at depths shallower than 100 m [*Fernández-Álamo and Färber-Lorda*, 2006; *Cepeda-Morales et al*., 2009, 2013], and the DIC concentration is greater than 2200 μmol kg^{-1} within 50 m of the surface [*Maske et al*., 2010]. The CO_2 flux in the OMZ of the NETP, however, has not yet been estimated and its contribution to the global carbon balance has not been defined. In this region, the coastal oxycline and carboncline occur at shallow depths, between 50 and 100 m [*Fernández-Álamo and Färber-Lorda*, 2006; *Cepeda-Morales et al*., 2009, 2013], with an inverse relationship between the oxycline depth and the surface pCO_2 value [*Maske et al*., 2010]. Many CO_2 flux studies have been carried out in the open ocean [*Takahashi et al*., 2009]. However, there are few in conjunction with coastal OMZ, including the NETP off Mexico. Due to the lack of studies in the NETP OMZ, there is an ongoing debate as to whether this

region acts as a year-round source of CO_2, or whether it may also act as a carbon sink due to the high rates of productivity [*López-Sandoval et al*., 2009].

The objective of this study is to determine the primary processes affecting the air-sea CO_2 flux above the OMZ of the coastal NETP off Mexico. Fluxes were calculated during two temporal (seasonal) and spatial distributions of the OMZ, providing a breadth of different oceanographic conditions to investigate surface carbon dynamics.

2. Data and Methods

2.1. Data Collection and Analysis

Two oceanographic cruises were carried out in the NETP off Mexico: the first was from 18 to 30 November 2009 on board the R/V El Puma and covered 38 stations (Figures 1a and 1c); the second was from 3 to 31 August 2010 on board the Mexican Navy's R/V Altair and covered 85 stations (Figures 1b and 1c). During the November 2009 cruise, a SeaBird SBE-911 Plus CTD was used to measure temperature, conductivity, oxygen, and fluorescence to 1000 m depth. In addition, at several stations measurements were taken to 2000 m, or near the bottom at shallow stations. In August 2010, the same parameters were measured with a SeaBird SBE-19 Plus CTD to 500 m depth. For both cruises, the potential temperature (θ) and salinity (S) data were used to construct θ-S diagrams for defining regional water masses as proposed by *Fiedler and Talley* [2006], *Castro et al*. [2006], and *Lavín et al*. [2009].

Discrete water samples for DIC and total alkalinity (TA) were collected at 19 stations in November (Figure 1a) and 30 stations in August (Figure 1b). During November 2009, 12 L Niskin bottles mounted on a rosette were closed at 12 depths to 1000 m. During August 2010, six depths were sampled to 200 m with 5 L Niskin bottles attached to a hydrographic wire using a messenger. Seawater was stored in 500 mL borosilicate bottles and preserved with 100 μL of a saturated solution of mercuric chloride ($HgCl_2$). The bottles were sealed with Apiezon grease to prevent evaporation and contact with the atmosphere.

DIC was measured following the coulometric method described by *Johnson et al*. [1987]. Prior to the analysis, accuracy and precision were assessed using certified reference material for DIC provided by Dr. Andrew Dickson from Scripps Institution of Oceanography [*Dickson et al*., 2003]. Reference material gave an average difference relative to the certified value of 1.5 ± 1.1 μmol kg^{-1}, with a maximum of 4 μmol kg^{-1}; a measurement error of 0.2%.

The potentiometric method described by *Dickson et al*. [2003] was used to measure TA. Reference standards were used for the measurements and the differences relative to the certified value were not greater than 5 μmol kg^{-1} (with an average of 2.0 ± 1.5 μmol kg^{-1}), indicating a measurement error of 0.2%. The altimeter data analyzed in this study (to determine sea surface height) are the high-resolution sea level anomalies distributed by Ssalto/Duacs at 7 day intervals on a 1/3° Mercator grid, objectively interpolated onto a uniform 1/4° grid and referenced to a relative 7 year mean (1993–1999) (http://www.aviso.oceanobs.com) [*Ducet et al*., 2000; *Le Traon et al*., 2003]. The data extend from October 1992 to October 2010 and represent the updated multimission gridded product referred by AVISO (The Archiving, Validation, and Interpretation of Satellite Oceanographic) as the "Delay Time maps of sea level anomaly (DT-mslaupd)." The geostrophic velocities for the period comprising the cruises were calculated from sea surface height (SSH) fields.

2.2. Data Processing

For the November 2009 survey, the oxygen data were calibrated with discrete samples taken at 10, 100, and 450 m for the profiles were carbon data were collected. The oxygen samples were measured following the World Ocean Circulation Experiment (WOCE) Operations Manual (http://cchdo.ucsd.edu/manuals.html). Percent oxygen saturation was calculated using the Ocean Data View software [Schlitzer, R., Ocean Data View, http://odv.awi.de, 2013], which uses the method proposed by *Weiss* [1970].

Oxycline depth for every profile was defined as described by *Maske et al*. [2010], using the depth of maximum oxygen difference over 4 m depth calculated for every meter: $\Delta[O]/m = ([O]_{z-2} - [O]_{z+-2}])/4$, where Z is depth in meters until the maximum gradient was determined.

To eliminate the effects of evaporation or precipitation of freshwater for surface data, the DIC and TA measurements were normalized as described by *Friis et al*. [2003]. This method considers an end member for DIC different from zero when $S = 0$ ($DIC^{S=0}$). The following normalization equation was used:

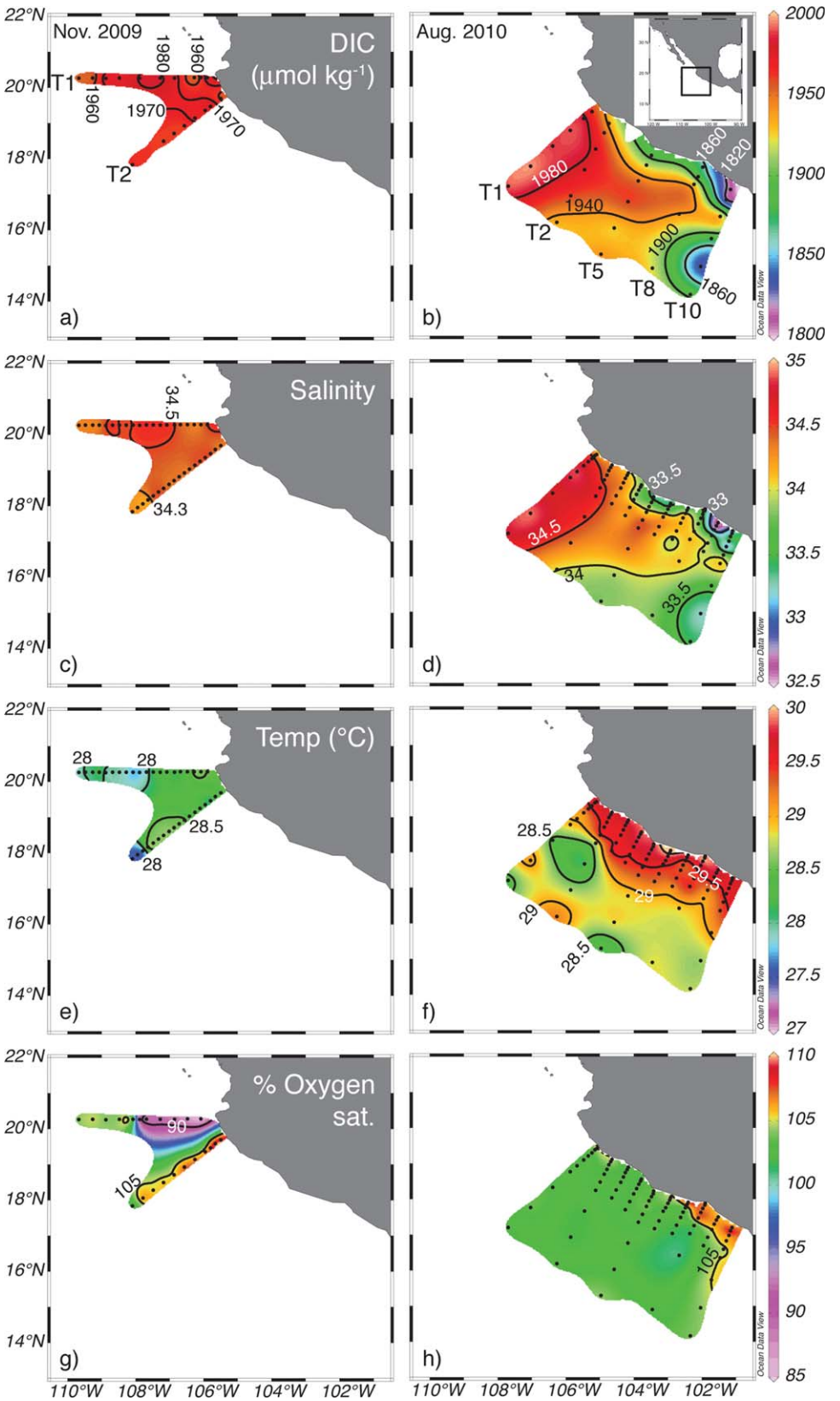

Figure 1. Distribution of (a and b) dissolved Inorganic carbon (DIC), (c and d) salinity, (e and f) temperature (°C), and (g and h) % oxygen saturation at 10 m depth during the cruises conducted in (left) November 2009 and (right) August 2010. The primary transects (T) are indicated.

$$\mathrm{NDIC} = \left[\left(\mathrm{DIC}_{\mathrm{measured}} - \mathrm{DIC}^{S=0}\right)/S_{\mathrm{measured}}\right] * S_{\mathrm{reference}} + \mathrm{DIC}^{S=0},$$

where NDIC is the normalized DIC concentration, $S_{measured}$ is the measured salinity for the sample, and $S_{reference}$ is a reference salinity. The mean salinity value for the upper 30 m for both surveys was used as the reference salinity value (34.29). To obtain $DIC^{S=0}$, a multiple linear regression was used to fit the surface layer (<30 m) values of temperature (T), salinity (S), and DIC to the equation:

$$\mathrm{DIC} = {}_{mT}\mathrm{T} + {}_{ms}\mathrm{S} + b_0,$$

where $b_0 = DIC^{S=0}$. The regression yielded:

$$\mathrm{DIC} = -4.5(\pm 1.0)\mathrm{T} + 80(\pm 2.5)\mathrm{S} - 680(\pm 98)$$

thus $DIC^{S=0} = -680(\pm 98)$.

In situ pH (seawater scale) and pCO_2 were calculated using the CO2Sys.xls program [*Lewis and Wallace*, 1998] from discrete DIC and TA measurements with an accuracy of ±5 μatm for pCO_2 (<2%) and ±0.01 for pH. The dissociation constants of *Mehrbach et al*. [1973] as refitted by *Dickson and Millero* [1987] were used for the calculations. Calcium concentration was considered conservative and calculated based on salinity.

CO2Sys.xls was also used to calculate DIC and pH (seawater scale) in equilibrium with the atmosphere using the atmospheric pCO_2 for the date and sampling latitude (~387 μatm) [*GLOBALVIEW-CO2*, 2013, http://www.esrl.noaa.gov/gmd/ccgg/globalview/co2/co2_intro.html), and average surface TA. The estimated DIC and pH in equilibrium with the atmosphere were 1968 (±6) μmol kg^{-1} and 8.04 (±0.01), respectively.

The stratification parameter (Φ) was calculated according to *Simpson* [1981]. It is expressed in J m^{-3} and represents the amount of work per volume needed to mix the water column to a specified depth (in this case, 300 m).

2.3. Calculation of Air-Sea CO_2 Flux

The air-sea CO_2 fluxes (FCO_2) were calculated using the formulation $FCO_2 = K\alpha(\Delta pCO_2)$, where K is the gas transfer velocity; α is the solubility of CO_2 in seawater, estimated based on in situ salinity and temperature [*Weiss*, 1974]; and ΔpCO_2 is the difference between the partial pressure of CO_2 in the water and atmosphere ($\Delta pCO_2 = pCO_{2water} - pCO_{2atm}$). A pCO_{2atm} of 387 μatm was used for the sampling date and latitude [*GLOBALVIEW-CO2*, 2013]. K is parameterized as a function of wind velocity following *Wanninkhof* [1992, equation (3)]. Wind data used were a cross calibrated, multiplatform ocean surface wind velocity product (CCMP) obtained from http://podaac.jpl.nasa.gov/DATA_CATALOG/ccmpinfo.html, with resolution of four data points per day and 0.25 × 0.25 latitude/longitude. This data set is a gridded product obtained from combining remote sensed wind data, cross calibrated with available conventional ship and buoy data as described in *Atlas et al*. [2011]. Differences between CCMP analyses and wind observations are small, approximately 0.5 m s^{-1}. The wind speed data were linearly interpolated to the date and sampling position shown in Figure 1. Positive FCO_2 values indicate a gas flux from the sea to the atmosphere, whereas negative values indicate a flux from the atmosphere to the sea.

As the calculation of pCO_{2water} had an error of ±5 μatm, the error associated with the FCO_2 estimation is ±0.1 mmol C m^{-2} d^{-1} when wind speed was low (<2.5 m s^{-1}) and ±0.9 mmol C m^{-2} d^{-1} when wind speed was high (6–8 m s^{-1}).

3. Results

The work presented here examines the primary physical and biogeochemical mechanisms controlling the air-sea CO_2 fluxes in the NETP off Mexico for two different oceanographic conditions: November 2009 and August 2010. Additionally, El Niño and La Niña conditions occurred during the first and second cruise, respectively (NOAA; http://www.esrl.noaa.gov/psd/enso/mei/#ElNino). First, the distribution of DIC, salinity, temperature, and % oxygen saturation in surface waters are described, then the air-sea CO_2 fluxes, and finally the water masses and associated pCO_2 values are presented.

3.1. Surface Distribution

Similar distributions for surface DIC and salinity were observed during each survey. In November 2009, DIC values at 10 m ranged from 1950 to 1980 μmol kg^{-1} (Figure 1a). The highest values (1980 μmol kg^{-1}) coincided with the maximum salinity value of 34.55 (Figure 1c), and were observed along T1 ($\sim$107°W). The lowest DIC concentrations ($<$1960 μmol kg^{-1}) were found in areas with salinity $<$34.35, at the stations farther offshore at both (T1 and T2) and in the nearshore stations of T2. For the November cruise, the mean DIC concentration at 10 m was 1966 $\pm$ 9 μmol kg^{-1}.

Distribution of temperature at 10 m during November 2009 is shown in Figure 1e. Mean temperature was 28.1 $\pm$ 0.3°C and did not vary greatly over the study area. The highest values (28.5°C) were observed at the stations closest to coast and in the middle of T2 ($\sim$107°W), while the lowest values (27.5°C) were observed at the oceanic stations for both transects.

The spatial pattern of the above variables at 10 m depth showed maximum values in the middle part of T1 (except for temperature), and minimum values at the offshore stations of T1 and T2. A different distribution pattern was observed in percent oxygen saturation at 10 m (Figure 1g): low oxygen saturation values (85–100%) were registered in the middle of T1 and toward the coast, while high values (105–110%) were observed at the oceanic stations of T1 and throughout T2.

During August 2010 a north-south concentration gradient was observed in the surface distribution of DIC (Figure 1b) and salinity (Figure 1d), with a decrease of $\sim$170 μmol kg^{-1} and 1 U, respectively. Water with high DIC concentration (1940–1980 μmol kg^{-1}) and salinity values (34.00–34.90) was observed in the northern and central transects, suggesting an equatorward intrusion of high salinity water. The lowest DIC concentrations ($<$1900 μmol kg^{-1}) were measured in the southern region of the study area, with values as low as 1810 μmol kg^{-1} at the stations closest to the coast of T10. Also, in this southern region the lowest salinity values ($<$33.50) were found.

Temperature was slightly higher (up to 2.0°C) during August 2010 (Figure 1f) than in November 2009. Values ranged from 30.1°C in coastal areas to 28.1°C offshore. The 29°C isotherm divided the surveyed area into oceanic and coastal regions. Unlike salinity, there was no north-south gradient for temperature in this campaign.

Surface oxygen saturation during the August 2010 survey fluctuated between 110% and 100% (Figure 1h), unlike November 2009 where values below 100% were not observed. The highest values (110%) were measured in the southern sector of the study area at the nearshore stations of T10. The lowest DIC and salinity values were also found at the nearshore stations along T10. In the rest of the study area, the values were similar and close to saturation (100%).

3.2. CO_2 Flux

Previous ΔpCO_2 and FCO_2 analysis in the study region has excluded measurements made from coastal regions ($<$200 km) or during El Niño conditions [*Takahashi et al.*, 2002, 2009]. The first FCO_2 calculated for the coastal zone in the OMZ off Mexico are presented in this section. Differences between our findings and fluxes calculated in other OMZs will be discussed in section 4.3. Positive ΔpCO_2 (Figures 2a and 2b) and FCO_2 values (Figures 2c and 2d) were obtained in most of the study area for both cruises, except in the southernmost part of the area surveyed in August 2010, where negative FCO_2 were found (Figure 2d). In November 2009, FCO_2 ranged from $-$0.4 to 2.5 mmol C m^{-2} d^{-1} (Figure 2c), and most stations exhibited positive fluxes, indicating that the region acted as a weak source of CO_2. The highest ΔpCO_2 values and FCO_2 (30 μatm and 2.5 mmol C m^{-2} d^{-1}, respectively) were measured along T1, approximately 200 km from the coast ($\sim$107°W). Similar values were also observed at $\sim$106°W along T2, 120 km offshore. The lowest FCO_2 ($-$0.4 mmol C m^{-2} d^{-1}) were observed in the oceanic area of T1, where ΔpCO_2 was as low as $-$7 μatm. The nearshore stations were close to equilibrium in both transects.

A wider range of ΔpCO_2 and flux values was observed in August 2010 (Figures 2b and 2d) than in November 2009, ranging from $-$80 to 70 μatm and $-$4.4 to 3.3 mmol C m^{-2} d^{-1}, respectively. The highest ΔpCO_2 values (70 μatm; Figure 2b) were observed in the northern part of the study area and at the oceanic stations of T5, along with the highest FCO_2 values (2.7–3.3 mmol C m^{-2} d^{-1}; Figure 2d). Negative or near-equilibrium values occurred along the southern transects (T8 to T10) and at the stations closest to the coast (Figure 2d). The lowest ΔpCO_2 values ($-$80 to 0 μatm) were observed between T8 and T10. Also, the lowest

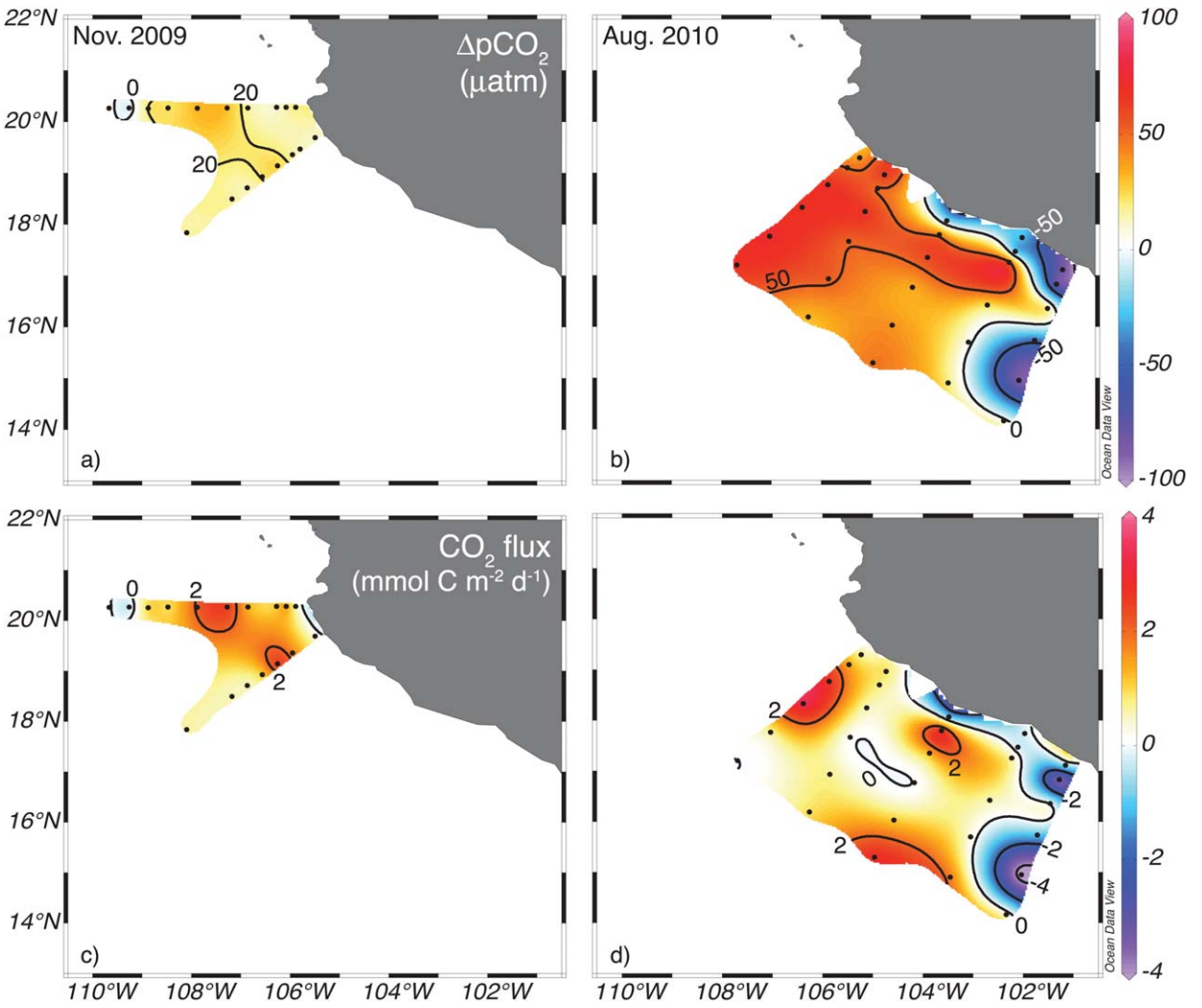

Figure 2. Surface distribution of sea-air pCO_2 differences (ΔpCO_2) in μatm for (a) November 2009 and (b) August 2010. Distribution of sea-air CO_2 flux (mmol C m^{-2} d^{-1}) for (c) November 2009 and (d) August 2010 surveys, calculated using the gas transfer coefficient of *Wanninkhof* [1992]. Values below zero (green to purple tones) indicate that the area can act as a carbon sink.

FCO_2 values (−3.8 and −4.4 mmol C m^{-2} d^{-1}) were found at the offshore stations of T10. There was a ∼150 μatm difference between ΔpCO_2 in the northern and southern regions of the study area.

3.3. Water Masses and Stratification

Four water masses were detected during both surveys, each with a characteristic pCO_2 value as shown in the θ–S diagrams (Figure 3). Tropical Surface Water (TSW) and Subtropical Subsurface Water (StSsW) were observed over the first 500 m of the water column. Also, a minor influence of California Current Water (CCW) was detected at the offshore, northernmost stations. Below StSsW and CCW (when present), Pacific Intermediate Water (PIW) occurred. The mean depths at which the water masses were detected, as well as their potential temperature, salinity, and pCO_2 values are shown in Table 1. Subarctic Water (SAW) and Gulf of California Water (GCW) were not detected; however their presence has been reported at the northern end of the study region [*Cepeda-Morales et al.*, 2013].

In both surveys, TSW was found from the surface to an average depth of 70 ± 10 m. The lower limit of this water mass was ∼10 m deeper in the stations sampled in November 2009 (84 ± 8 m) than August 2010 (69 ± 7 m). The average pCO_2 value for this water mass was 560 ± 260 μatm for both surveys. TSW with a salinity higher than 34.5 was identified in the northern transects of the August 2010 cruise (Figure 1d) and at some stations during November 2009 (T1 at ∼107°W; Figure 1c). In these regions, surface pCO_2 values

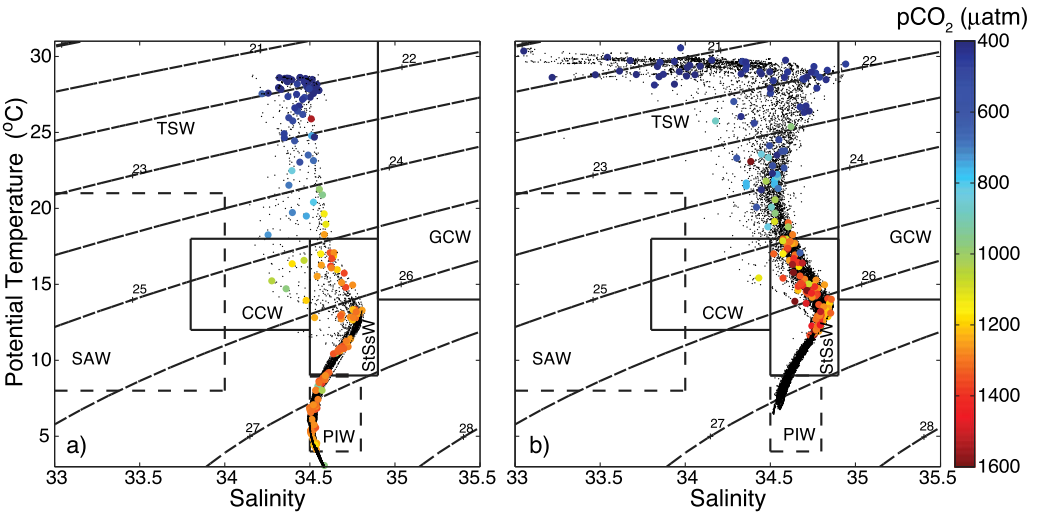

Figure 3. Potential temperature (θ) and salinity diagram for cruises conducted in (a) November and (b) August 2010. θ–S diagram for August shows the upper 500 m of the water column. The color bar indicates the pCO_2 value for each temperature and salinity measurement. TSW = Tropical Surface Water, StSsW = Subtropical Subsurface Water, GCW = Gulf of California Water, CCW = California Current Water, SAW = Subarctic Water, and PIW = Pacific Intermediate Water. Water masses were classified according to *Fiedler and Talley* [2006] and *León-Chavez et al*. [2010].

were ~100 μatm higher than in the regions where fresher TSW (salinity < 33.5) was found (Figures 2c and 2d) and resulted in positive CO_2 fluxes (Figures 2a and 2b). In August TSW with salinity <34.5 most commonly occurred from the central to the southern region following the salinity gradient (Figure 1d).

Typical stratification values from the NETP [*Fiedler et al*., 2013] were found in the region covered during the November 2009 cruise (>1200 J m^{-3}, Figure 4a) and in the coastal zone of the August 2010 cruise (Figure 4b). During August 2010 more weakly stratified regions (<1100 J m^{-3}) were found along T1, and at the more oceanic stations of T5, T8, and T10. For this cruise, the calculated mean was 1120 ± 110 J m^{-3}, while during the November 2009 cruise the mean was 1230 ± 80 J m^{-3}.

Temporally, a difference in stratification values of ~200 J m^{-3} was observed between the southernmost transect of November 2009 (T2) and the northernmost transect from August 2010 (T1), the first one being ~50 km farther north from the latter. Vertical distributions of temperature, potential density anomaly, oxygen, and pCO_2 for T1 and T2 are shown in Figure 5. The differences in density fields between T2 from November 2009 (Figure 5a) and T1 from August 2010 (Figure 5b) are consistent with the higher stratification values observed during November 2009 (~1200 J m^{-3}) compared to August 2010 (~1000 J m^{-3}).

The upper limit of StSsW was characterized by a potential density anomaly of 25 kg m^{-3} (white squares, Figures 5a and 5b). Along T2 from November 2009, StSsW was found at ~90 m (Figure 5a). At the stations close to the coast, however, the upper limit of this water mass was shallower (~70 m), with lower stratification values (<1180 J m^{-3}; Figure 4a). Oxygen concentration decreased to less than 20 μmol/kg at this depth

Table 1. Physical Characteristics of the Water Masses Detected in the Study Region[a]

Water Mass	Cruise	Upper Limit (m)	Lower Limit (m)	Temperature (°C)	Salinity	pCO_2 (µatm)
Tropical Surface Water (TSW)	9 Nov		84 ± 8	25.70 ± 3.30	34.40 ± 0.09	540 ± 230
(T ≤ 18, S < 34.9)	10 Aug		69 ± 7	25.70 ± 4.00	34.40 ± 0.36	580 ± 280
	Mean		70 ± 10			560 ± 260
Subtropical Subsurface Water (StSsW)	9 Nov	91 ± 13	419 ± 21	11.60 ± 1.80	34.69 ± 0.07	1290 ± 70
(9 ≤ T ≤ 18, 34.5 ≤ S ≤ 34.9)	10 Aug	70 ± 7		11.95 ± 1.95	34.72 ± 0.06	1340 ± 180
	Mean	77 ± 14				

[a]Mean values are given for each water mass. In the August 2010 survey, the profiles did not cover the total volume occupied by Subtropical Subsurface Water (StSsW) so the lower limit and mean pCO_2 is not reported. Mean temperature, salinity, and pCO_2 for this survey should be taken with caution. Pacific Intermediate Water and California Current Water are not included due to scarce data.

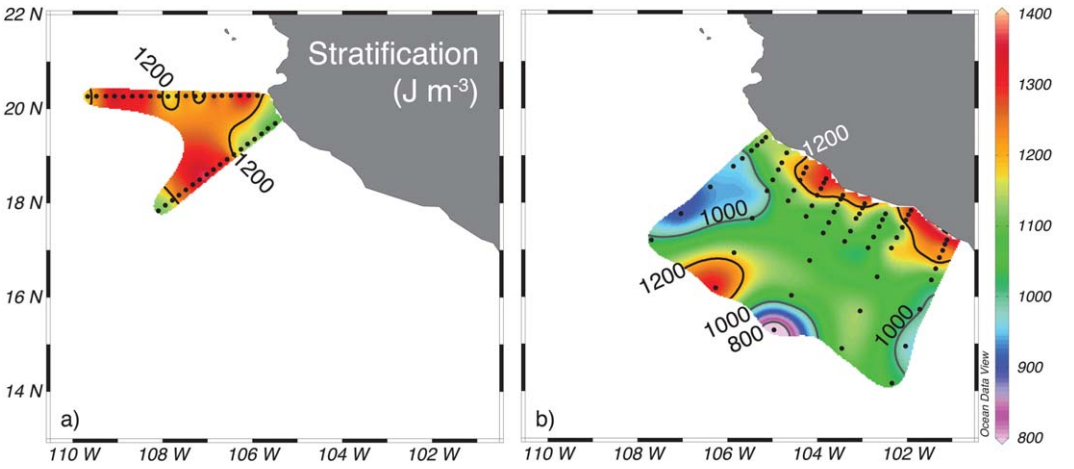

Figure 4. Stratification (J m^{-3}) calculated for the first 300 m for (a) November 2009 and (b) August 2010.

(Figure 5c), and a pCO_2 value of ~1200 μatm was found (Figure 5e), which implies an increase of ~800 μatm from the surface to the StSsW upper limit (a gradient of 9 μatm m^{-1}).

Along T1 from August 2010, the StSsW upper limit was identified at ~70 m (Figure 5b). That was 20 m shallower than in T2 from November 2009, except on the coastal region. Additionally, the oxygen concentration of 20 μmol kg^{-1} was ~30 m shallower than in the T2 from November 2009. Immediately below the oxygen concentration of 20 μmol kg^{-1}, pCO_2 values higher than 1400 μatm were observed. Similar pCO_2 values were not observed during November 2009.

Along the other transects (and contrary to what was observed in November 2009), StSsW was present ~20 m shallower at the oceanic stations (up to 50 m depth) than in the nearshore stations. This reflects differences in stratification between the oceanic and coastal region (Figure 4b) especially in the southern part of

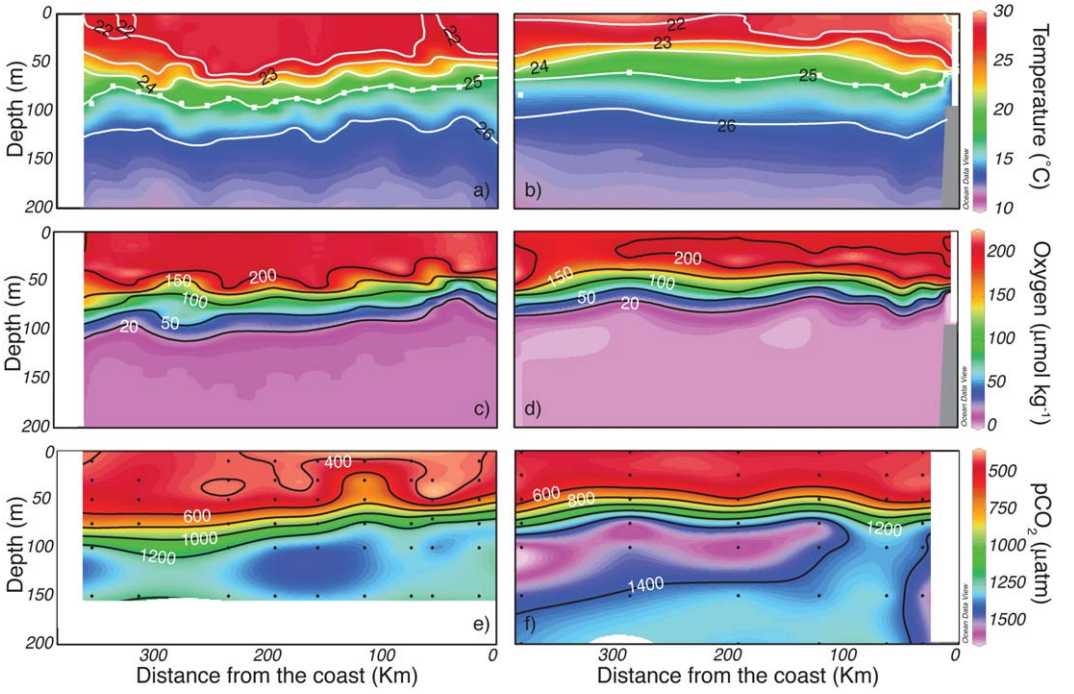

Figure 5. Vertical distribution of temperature (colors) and potential density (a and b) contours, (c and d) oxygen, and (e and f) pCO_2 along T2 in (left) November 2009 and T1 in (right) August 2010. White squares indicate the upper limit of StSsW, black dots indicate discrete sample locations.

the survey along T10. The pCO_2 found at the upper limit of StSsW and the mean pCO_2 value for the whole survey (1280 $\pm$ 180 μatm) were similar to the values during November 2009 at this depth; as well as for the whole water mass in both surveys (Table 1).

4. Discussion

In the NETP off Mexico, the oxycline depth and upper limit for the OMZ are associated with StSsW [*Cepeda-Morales et al*., 2013], where changes in this water mass depth may be driven by interannual, seasonal, and local phenomena that affect vertical mixing [*Maske et al*., 2010; *Cepeda-Morales et al*., 2013]. The high productivity of the region leads to significant organic matter remineralization at the oxycline and within the OMZ core, therefore producing DIC [*Paulmier et al*., 2006], increasing pCO_2, and helping to maintain the OMZ [*Paulmier et al*., 2006, 2011].

Due to the fact that shallow (~80 m) StSsW is characterized by high pCO_2 values (mean 1300 $\pm$ 180 μatm; Table 1), we analyze the influence of this water mass on the surface values of pCO_2 and FCO_2. Several physical phenomena, such as upwelling and mesoscale eddies that could influence the FCO_2 are considered. But first, the surface distributions of DIC and salinity are examined in order to understand the influence of advection on the spatial patterns of DIC and consequently pCO_2 and FCO_2.

4.1. Spatial Variability

The water masses detected in the upper 500 m of the water column (TSW and StSsW) were consistent with those reported by other authors for the region [*Fiedler and Talley*, 2006; *Kessler*, 2006; *León-Chávez et al*., 2009; *Cepeda-Morales et al.,* 2013]. Additionally, in both surveys subsurface salinity and temperature (between the isopycnal surface of 24.5 and 26.2 kg m^{-3}; Figure 3) were lower at the offshore stations (T1 and T2 from November, only in T1 for August) due to influence from the California Current which carries more oxygenated water to the northern end of the study [*Cepeda-Morales et al*., 2013]. Surface salinity during the November 2009 survey (34.3–34.6; Figure 1c) was consistent with mean seasonal climatology values for fall reported by *Fiedler and Talley* [2006]. Surface temperature, however, was up to 0.5°C higher than climatology values for the same season.

During August 2010, surface salinity along the northern transects was ~34.9, which is consistent with mean summer values for the region [*Fiedler and Talley*, 2006]. Although, surface salinity found on the southern end of the survey (<33.5), was as much as one unit lower compared with climatology data. The north-south salinity gradient (Figure 1d) may be attributed to a summertime intensification of the pole-ward Mexican Coastal Current (MCC). The MCC carries fresher TSW with low salinity (~33.5) and high temperature (>29°C) to the study region [*Lavín et al*., 2006; *Kessler*, 2006]. TSW surface water mass is formed in the tropics where precipitation is greater than evaporation [*Fielder and Talley*, 2006]. Furthermore, the influence of freshwater from the Balsas River which flows into the coastal region of T9 may have contributed to a decrease in salinity [*De la Lanza-Espino et al*., 2004] of the stations closest to the coast (3 km).

The NETP off Mexico is a transition zone [*Fiedler and Talley*, 2006; *Roden*, 1971], where more saline (>34.5) TSW was identified in some stations of the survey in November 2009 (Figure 1c) and in the northern region for August 2010 (Figure 1d). TSW with these characteristics has been called modified or evaporated TSW (mTSW) to indicate a transitional condition [*León-Chávez et al*., 2009]. This high-salinity TSW could partially be the result of mixed TSW and Gulf of California Water (S > 34.9), which has been observed in previous work in the study region [*Cepeda-Morales et al*., 2013].

Variation in pCO_2 can result from changes in DIC and TA concentration [*Sarmiento and Gruber*, 2006]; therefore, surface DIC data were analyzed with respect to surface salinity (Figure 6, open circles). A strong relationship was observed between these two variables ($r^2 = 0.95$, $n = 48$, $p < 0.001$). The DIC values in the present study were consistent with data collected along WOCE transect P18 in April 1994 [*Feely et al*., 1994]; however, we found lower concentrations (~80 μmol kg^{-1} lower) relative to P18. The lower concentrations may be because our data were collected closer to the coast and some stations may have been influenced by biological carbon consumption (see below). Also, DIC concentration can be affected by physical processes such as evaporation, precipitation, upwelling, and/or mixing of water masses [*Sarmiento and Gruber*, 2006].

To examine whether the observed spatial variability of DIC (Figures 1a and 1b) was associated with physical processes, DIC was normalized as mentioned in section 2.2. Upon normalizing the data the gradient disappears (crosses, Figure 6). Since no evidence of upwelling was found in the surface layer (see below), we

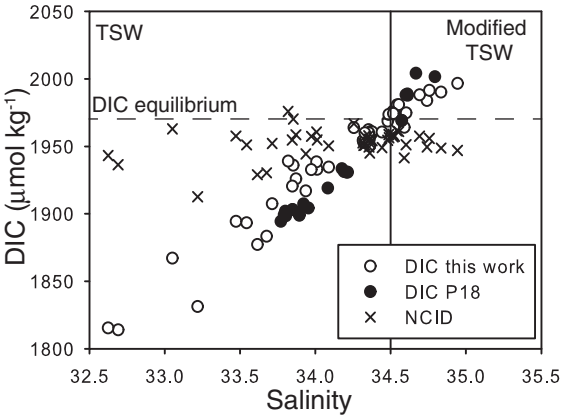

Figure 6. Surface dissolved inorganic carbon (DIC) measured in the present study versus surface salinity ($r^2 = 0.95$, $n = 48$). Also shown are DIC measurements of transect P18 from the World Ocean Circulation Experiment (WOCE) and salinity-normalized DIC (NDIC; S = 34.294). Equilibrium DIC is the expected surface DIC value when surface waters are in equilibrium with the atmosphere (1968 ± 8 μmol kg^{-1}).

propose that the distribution of surface DIC and pCO_2 was largely controlled by horizontal advection, and possibly evaporation of TSW given the highly stratified surface layer (Figure 4). TSW originates close to the Equator, a region with high rainfall, but its salinity and chemical properties may be modified in transition zones such as the NETP off Mexico. Furthermore, the evaporation of TSW causes concentration of chemical components such as DIC and salinity.

The solubility of gases decreases as water temperature increases, favoring an increase in pCO_2 in surface waters. To eliminate this effect the correction proposed by *Takahashi et al.* [1993] was applied. The temperature-induced changes in pCO_2 were found to be minimal (up to ±10 μatm; data not shown) and the distribution gradient shown in Figures 2a and 2b remained.

Advection of surface water masses largely determined DIC concentration and thus the value of surface pCO_2. Nonetheless, high values of primary productivity have been reported for the region (up to 447 mg C m^{-2} d^{-1}); particularly during the summer [*López-Sandoval et al.*, 2009]. Given that inorganic carbon consumption during photosynthesis favors an increase in pH [*Simpson and Zirino*, 1980; *Zirino and Lieberman*, 1985]; the in situ pH (Figure 7) was taken as first approximation for the "productivity footprint" for the August 2010 survey.

High values of pH (>8.04; Figure 7) were found in three regions in August 2010: the coastal zone, the oceanic region of T2, and along T10, where the lowest DIC concentration (Figure 1b), ΔpCO_2, and FCO_2 values occurred (Figures 2b and 2d). These results suggest that in these three regions inorganic carbon uptake by phytoplankton, in addition to CO_2 evasion, may have also contributed to a decrease in surface DIC and therefore to low positive or negative FCO_2.

4.2. Temporal Variability

During November 2009, temperatures were up to 0.5°C higher than those reported in climatologies (27–28°C) for the fall in the area. This may be due to El Niño influence, since variability of this magnitude has previously been reported for this region [*Fiedler and Talley*, 2006]. The maximum surface temperatures (~30°C), however, for both surveys were detected in the coastal zone in August (Figure 1f), which is typical for the region and the season.

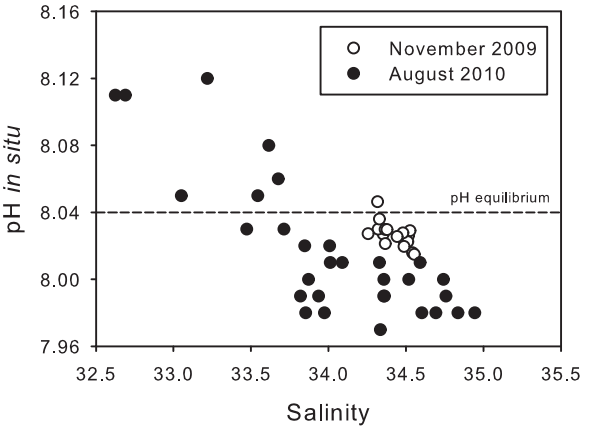

Figure 7. In situ pH (total proton scale) versus salinity. Data from the first 10 m are shown. Also the value of pH in equilibrium with the atmosphere (8.04) is indicated.

Sea surface height anomalies (SSHA) and the derived geostrophic velocities for the time of both surveys are shown in Figure 8. *Godínez et al.* [2010] reported that during November 2005 (a non-El Niño year), the SSH gradient was directed onshore producing favorable upwelling conditions. On the other hand, the climatological coastal upwelling index shows values which favor upwelling from January to June [*Kurczyn et al.*, 2012, Figure 12c].

During the November 2009 cruise, upwelling favorable winds (north-northwest) prevailed during the time of the survey. The isopycnals were found ~25 m shallower near the coast (Figure 5a), and values for stratification were ~80 J m^{-3} lower in the coastal regions than

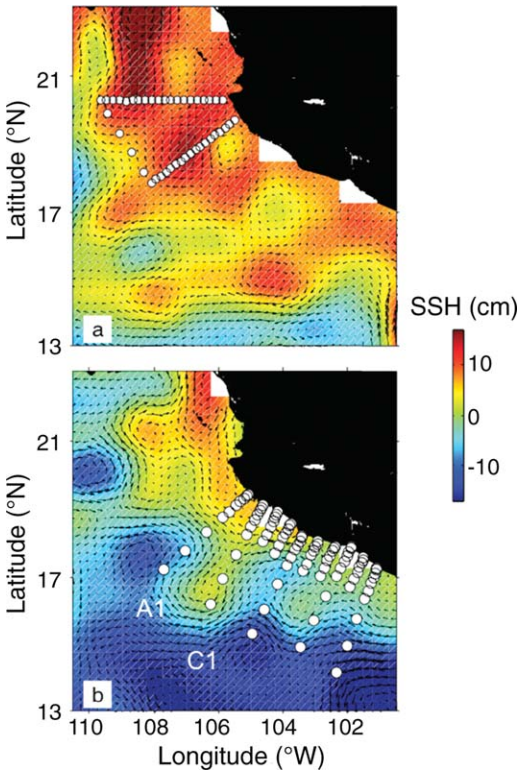

Figure 8. Sea surface height anomaly (SSHA) for (a) November 2009 and (b) August 2010. These satellite images correspond to the days when the cruises were conducted. White points indicate the location of the sampling stations. The locations of a cyclonic eddy (C1) and anticyclonic eddy (A1) are shown.

in the oceanic stations. Despite the above, evidence of upwelling was not observed in the surface (i.e., lower surface temperature, lower SSH on the coast). A possible explanation is the combination of effects of the seasonal variability and an El Niño event; both of which favor the development of higher sea level in the region [*Godínez et al*., 2010] and may have prevented this particular upwelling event from bringing StSsW water with high pCO_2 values (Table 1) to the surface.

During August 2010, warm water (>29°C) accumulation was observed at nearshore stations (Figures 1f) and downwelling favorable wind direction (south-southeast) was observed. This is consistent with the monthly climatology upwelling index for September [*Kurczyn et al*., 2012], and with the positive SSHA near the coast in Figure 8b. The SSHA field observed for August 2010 was influenced by the seasonal signal and interannual effect of La Niña (NOAA; http://www.esrl.noaa.gov/psd/enso/mei/-El Nino). La Niña events in the tropical Pacific cause negative SSH anomalies [*Godínez et al*., 2010]. The seasonal signal that causes maximum SSH near the coast during August and September (primarily due to the MCC) may explain up to 50% of the total variance in the area [*Godínez et al*., 2010]. Although influence of La Niña on SSHA cannot be discarded, the observed higher temperatures and positive SSH anomalies near the coast more likely represent a seasonal effect rather than interannual variability by La Niña.

Figure 9 shows the potential density anomaly (σ_θ) vertical profiles for both surveys as well as discrete pCO_2 values. Water from the OMZ with high pCO_2 values (1290 $\pm$ 70 μatm; Table 1) occurred below the oxycline and at σ_θ greater than 25 kg m^{-3} (StSsW upper limit; Figures 3, 5a, and 5b). Increased depth of this water mass is expected to cause decreased DIC input from the OMZ, therefore decreasing ΔpCO_2 and affecting FCO_2 direction at the surface. Conversely, increased DIC input to the surface is expected if the StSsW upper limit is found at shallower depths [*Maske et al*., 2010; *Paulmier et al*., 2008, 2011].

Despite the shallow upper limit of the OMZ, high stratification values (>1200 J m^{-3}) were determined for both surveys, particularly during November 2009 (Figure 4a). Stratification values were consistent with the climatology for the region presented by *Fiedler et al*. [2013]. Also, the influence of El Niño during November 2009 resulted in an increase in SSHA (Figure 8a), and is in agreement with results shown by *Filonov and Tereshchenko* [2000] in the same study area during the 1997–1998 El Niño. In November, the upper limit of StSsW was found between 75 and 95 m (Figure 9a) and up to 125 m at the oceanic station of T1. This station was influenced by CCW, where the upper limit of StSsW did not corresponded to 25 kg m^{-3}. ΔpCO_2 values at the surface showed little variability (16 $\pm$ 9 μatm), with a range between 30 (maximum) and -7 (minimum) μatm.

In August 2010, the StSsW upper limit was ~20 m shallower than in November 2009 (Figures 9b, 5a, 5b and Table 1). In this case, surface ΔpCO_2 varied greatly, from -80 to 80 μatm (Figure 2b). Moreover, during this cruise, the presence of cyclonic and anticyclonic eddies affected stratification, the depth of StSsW, and surface pCO_2 values. This is in agreement with results reported by *Godínez et al*. [2010] who mention that mesoscale phenomena may explain up to 50% of the variance of SSHA in offshore regions.

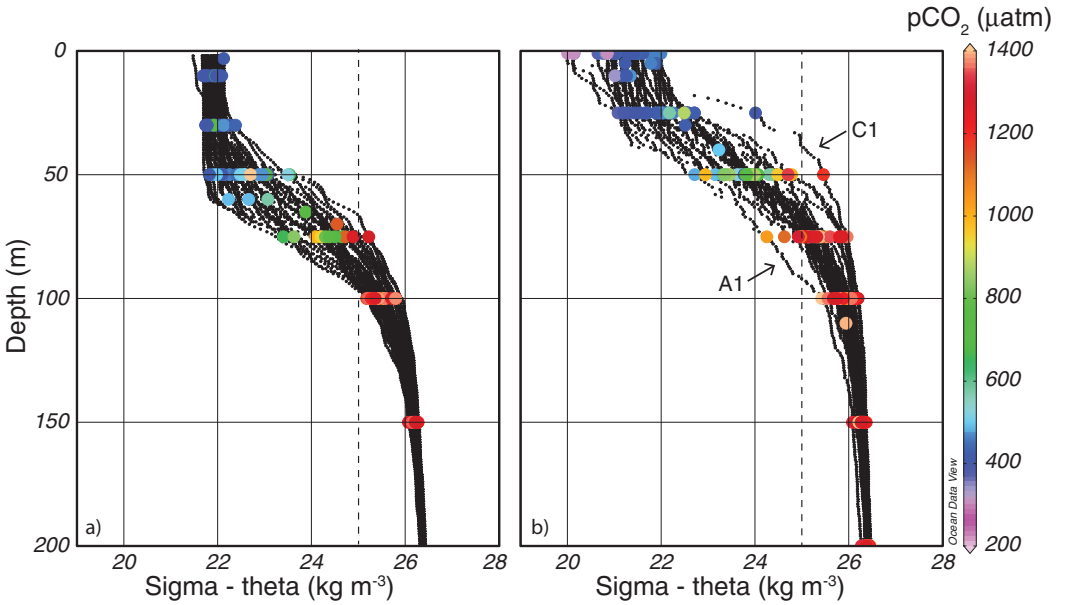

Figure 9. Potential density (σ_θ) anomaly profiles for all stations surveyed in (a) November 2009 and (b) August 2010. The color bar shows the pCO_2 (µatm). Density at the upper limit of StSsW is indicated (25 kg/m^3).

The cyclonic eddy mentioned above was detected at the farther offshore stations of T5 (C1; Figure 8b), where the upper limit of StSsW was 20 m shallower (at ~40 m; top profile in Figure 9b) than at all other stations. The influence from the eddy was reflected in the surface by a decrease in temperature of ~0.7°C (Figure 1f) and an increase of ~13 μatm in seawater pCO_2; hence, the area acted as a CO_2 source during the study period, with a flux of 2.8 ± 0.9 mmol C m^{-2} d^{-1} (Figure 2d). The lowest stratification value was also observed here (~700 J m^{-3}), which is similar to values reported in upwelling regions such as the California Current and the Peru-Chile Current [*Fiedler et al.*, 2013].

The anticyclonic eddy detected in the oceanic area of T2 (A1, Figure 8b) increased the mixed layer depth by ~20 m (Figure 8b). Surface temperature in the region was ~0.5°C greater than surrounding waters (29.2°C; Figure 1f), and stratification was higher (>1200 J m^{-3}); similar to November 2009 values. No significant differences between stations along the same transect were observed for FCO_2 magnitude or direction.

Maske et al. [2010] reported that when the upper limit of the OMZ (or CMZ) is shallow, the influence on surface pCO_2 is greater and the ΔpCO_2 values tend to be positive (favoring evasion), whereas in regions where the oxycline is deeper, the ΔpCO_2 values are lower. In the present study, no significant relationship was found between surface ΔpCO_2 and either oxycline depth or StSsW upper limit depth ($r^2 < 0.1$; Figure 10). For example, a ΔpCO_2 value of 50 μatm was found with two different oxycline depths (30 and 70 m; Figure 10a). Furthermore, when the StSsW upper limit was ~60 m different ΔpCO_2 values were found to vary between −80 and 80 μatm (Figure 10b). Also, during August 2010, a region with ΔpCO_2 values between −20 and −80 μatm was found at the southern transects (Figure 2b). Consequently, the resulting FCO_2 were negative (~−4 mmol C m^{-2} d^{-1}, Figure 2d) even though the oxycline and StSsW were near the surface (less than 50 and 80 m, respectively).

Low correlation of subsurface water with ΔpCO_2 at the surface (Figure 10) and a strong relationship between surface DIC and salinity (Figure 6) shows that the dynamics of surface CO_2 were controlled by horizontal advection of water masses above the oxycline, and to a lesser extent, the influence of subsurface water from the OMZ.

4.3. CO_2 Flux

FCO_2 for November 2009 and August 2010 were lower than 5 mmol C m^{-2} d^{-1} (Figures 2c and 2d), which is the criterion to determine high CO_2 flux values proposed by *Paulmier et al.* [2008] based on the highest flux reported for the open ocean by *Takahashi et al.* [2002]. In fact, FCO_2 and ΔpCO_2 values reported here were highly comparable with those found in the open ocean off Mexico (>200 km from the coast) during non-El Niño years (Table 2). The highest FCO_2 observed along T1 and T2 (off Cabo Corrientes) for both surveys

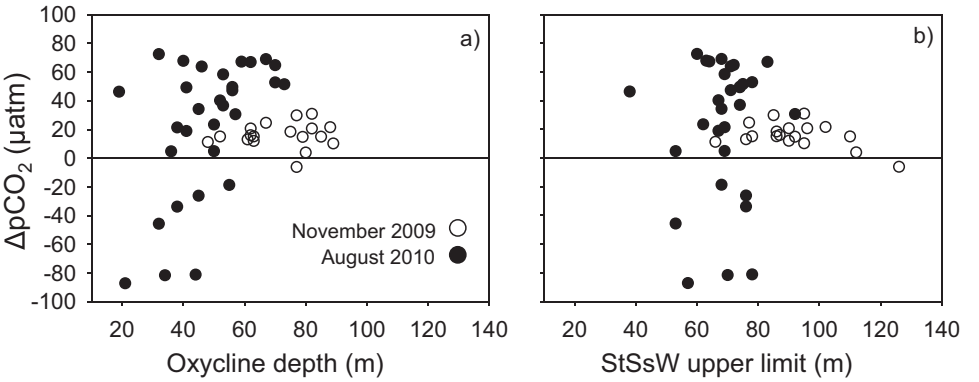

Figure 10. (a) The oxycline depth calculated as the maximum oxygen concentration gradient over 4 m and (b) StSsW upper limit versus surface ΔpCO_2 for both surveys. The horizontal black line indicates equilibrium with the reference atmospheric CO_2 (387 μatm). $r^2 < 0.1$ in both cases.

ranged from 2.5 to 3.3 ± 0.9 mmol C m^{-2} d^{-1}. Thus, this region acted as a weak carbon source while the southernmost sector surveyed acted as a carbon sink, with values ranging from −3.8 to −4.4 ± 0.1 mmol C m^{-2} d^{-1}. In this region, the high pH values (>8.04) suggest prior biological carbon consumption (Figure 7).

Surface water mass advection played an important role in defining whether an area acted as a carbon source or sink. The influence of fresher TSW (Figure 6) and biological carbon fixation (Figure 7) favored a negative ΔpCO_2, which results in an invasion of CO_2.

In general, lower FCO_2 than those reported for other OMZs (Table 2) were observed in the study area. FCO_2 of up to 18.8 mmol C m^2 d^{-1} has been reported for the OMZ of the northern Humboldt Current off Peru [*Friederich et al.*, 2008]. Reported fluxes for the northern Humboldt Current are up to 4 times greater than the values presented herein for the NETP off Mexico, indicating significantly different dynamics. The difference may be attributed to lower stratification due to intense upwelling that occurs in the OMZ off Peru year round, which transports subsurface waters with high concentrations of DIC to the surface. In the present study, seasonal variability of SSHA combined with the interannual El Niño signal in November 2009 produced strong stratification in the coastal areas; while in August 2010 the seasonal signal dominated over the La Niña condition in the coastal region, with accumulation of surface water with low DIC on the coast (Figure 1b). Though the StSsW was deeper in November 2009 due to the influence of El Niño, there were no large differences in FCO_2 magnitude relative to that observed in August 2010 except in the southern region (T8, T10) where negative FCO_2 occurred.

In this study, a mean wind speed of 5 ± 1 m s^{-1} was observed during the November 2009 cruise, however ΔpCO_2 values were low (Figure 2a) resulting in moderate CO_2 evasion in the region (Figure 2c). Although mean wind speed in the August 2010 survey was lower (mean 3 ± 2 m s^{-1}) compared with the November 2009 cruise, ΔpCO_2 values were higher (−80 to 80 μatm; Figure 2b), which favored an enhanced gas exchange with the atmosphere.

Finally, subsurface water with high DIC concentrations did not play a major role in controlling surface FCO_2 due to strong stratification found in the coastal NETP off Mexico. Rather, the advection of surface water

Table 2. Sea-Air CO_2 Fluxes Reported for Other Regions[a]

Region	Sea-Air CO_2 Flux ± SD (mmol C m^{-2} d^{-1})	Reference
Baja California 26°N (Feb to May, minimum)	−2.7	*Hernández-Ayón et al.* [2010]
Open Ocean[b]	−1.08, 2.28	*Chavez et al.* [2007] and *Takahashi et al.* [2013]
OMZ off Peru (not upwelling)	6.9	*Friederich et al.* [2008]
Baja California 26°N (Jul to Nov, maximum)	8.3	*Hernández-Ayón et al.* [2010]
OMZ off Chile	9.1 ± 8.2	*Paulmier et al.* [2008]
OMZ off Peru (annual mean)	14.2 ± 9.8	*Friederich et al.* [2008]
OMZ Peru (upwelling, maximum)	27.8	*Friederich et al.* [2008]
OMZ Arabian Sea (upwelling, maximum)	119	*Kortzinger et al.* [1997]
OMZ Pacific off Mexico (minimum)	−4.4	This work
OMZ Pacific off Mexico (maximum)	3.3	This work

[a]All the studies compared here used the gas transfer coefficient from *Wanninkhof* [1992].
[b]Mean flux calculated based on 1.75 million measurements of pCO_2, excluding coastal zones, as well as measurements made in the Equatorial Pacific (10°N–10°S) during El Niño events.

masses and their productivity determined whether the region acted as a CO_2 source or sink. However, in view of the occurrence of StSsW at shallow depths, the influence of subsurface water transported to the surface by physical forcing cannot be discarded [*Maske et al*., 2010], as this could increase the region's capacity to act as a source of CO_2 to the atmosphere.

5. Conclusions

The coastal Tropical Pacific off Mexico is characterized by a prominent OMZ, where high values of pCO_2 (Figures 5e and 5f) occur below the oxycline, which is generally strong and shallow (~70 m). In this region, we expected to find a strong carbon source to the atmosphere (>5 mmol C m^{-2} d^{-1}), however, the region behaved only as a weak source (maximum FCO_2 of 3.3 mmol C m^{-2} d^{-1}). In addition previous studies have reported a negative relationship between the oxycline depth and the ΔpCO_2 value at the surface, indicating influence from the OMZ [*Maske et al*., 2010]. In the present study, however, we observed a large range of values on the surface (Figure 2), which resulted from the combination of diverse surface processes.

In most of the study region, tropical surface water (TSW) was found in the upper layer of the water column, and TSW with salinity >34.5 (known as modified TSW) was identified along the northern transects of both cruises. This region behaved as a weak carbon source to the atmosphere, however, FCO_2 values were 4 times lower than those reported for other OMZs. The southernmost region sampled in August 2010, behaved as a carbon sink due to low DIC concentration (1910 ± 45 μmol kg^{-1}) and low pCO_2 values (400 ± 50 μatm). These values were primarily influenced by the presence of diluted TSW (S < 34.5) and biological productivity which increased the pH measured up to 0.2 U over the equilibrium value with the atmosphere.

During November 2009 the oxycline and the upper limit of StSsW were found at a mean depth of 90 ± 13 m, with high stratification values (>1200 J m^{-3}) due to El Niño influence. There were no major FCO_2 differences at the surface with respect to August 2010, where StSsW was shallower (~70 m). Contrary to what has been reported for other OMZs (Northern Humboldt Current, Arabian Sea), the influence from the StSsW from the OMZ, with high pCO_2 values (1290 ± 70 μatm), was not observed for surface DIC and pCO_2 due to the strong stratification. In fact, influence of OMZ water on the surface was only observed at a station affected by a cyclonic eddy that brought subsurface water to the surface, slightly increasing the FCO_2.

Therefore, we conclude that the primary physical factor that controlled the distribution of surface pCO_2 and FCO_2 in the NETP off Mexico were the horizontal advection and mixing of surface water masses and strong stratification. StSsW with high values of pCO_2 could have an influence on the surface during mesoscale phenomena or upwelling events if El Niño conditions (deeper mixed layer and higher stratification) are not present.

Acknowledgments

The authors wish to thank the crew and officers of the Mexican Navy R/V Altair and the R/V El Puma. We are especially indebted to M.C. Roberto Roa-Mendoza from the Instituto Oceanográfico del Pacífico de la Sexta región naval, Manzanillo, Colima. This project was funded partially by SEP-CONACYT project "Investigaciones Oceanográficas del Sistema Frontal de Baja California" (CB-2008/103898, PI E.B.), "Presupuesto de carbón, distribución y adaptación fisiológicas del zooplancton en l zona del mínimo de oxigeno del Pacífico Tropical Mexicano" (CB-2006/62152-F, JFL) and by UABC program 403/1/C/33/15. We also acknowledge support from CONACyT and UABC sabbatical grants. Finally, we thank Janet J. Reimer for help with the revision of the grammar and English language.

References

Atlas, R., R. N. Hoffman, J. Ardizzone, S. M. Leidner, J. C. Jusem, D. K. Smith, and D. Gombos (2011), A cross-calibrated, multiplatform ocean surface wind velocity product for meteorological and oceanographic applications, *Bull. Am. Meteorol. Soc.*, *92*, 157–174, doi:10.1175/2010BAMS2946.1.

Castro, R., R. Durazo, A. Mascarenhas, C. A. Collins, and A. Trasviña (2006), Thermohaline variability and geostrophic circulation in the southern portion of the Gulf of California, *Deep Sea Res., Part I*, *53*, 188–200, doi:10.1016/j.dsr.2005.09.010.

Cepeda-Morales, J., E. Beier, G. Gaxiola-Castro, M. F. Lavín, and V. M. Godínez (2009), Effect of the oxygen minimum zone on the second chlorophyll maximum in the Eastern Tropical Pacific off Mexico, *Cienc. Mar.*, *35*(4), 389–403.

Cepeda-Morales, J., G. Gaxiola-Castro, E. Beier, and V. M. Godínez (2013), The mechanisms involved in defining the northern boundary of the shallow oxygen minimum zone in the eastern tropical Pacific Ocean off Mexico, *Deep Sea Res., Part I*, *76*, 1–12, doi:10.1016/j.dsr.2013.02.004.

Chavez, F. P., T. Takahashi, W.-J. Cai, G. Friederich, B. Hales, R. Wanninkhof, and R. A. Feely (2007), Coastal oceans, in *The First State of the Carbon Cycle Report (SOCCR): The North American Carbon Budget and Implications for the Global Carbon Cycle*, report by the U.S. Climate Change Science Program and the Subcommittee on Global Change Research, edited by A. W. King et al., pp. 157–166, Natl. Oceanic and Atmos. Admin., Natl. Clim. Data Cent., Asheville, N. C.

De la Lanza-Espino, G., I. Rodriguez-Penié, and S. Hernández-Pulido (2004), Spatiotemporal variation of phosphorus and the effect of local currents on its distribution in Petacalco Bay, Guerrero, Mexico, *Cienc. Mar.*, *30*(2), 311–322.

Dickson, A. G., and F. J. Millero (1987), A comparison of the equilibrium constants for the dissociation of carbonic acid in seawater media, *Deep Sea Res., Part A*, *34*(10), 1733–1743.

Dickson, A. G., J. D. Afghan, and G. C. Anderson (2003), Reference materials for oceanic CO_2 analysis: A method for the certification of total alkalinity, *Mar. Chem.*, *80*, 185–197.

Ducet, N., P. Y. Le Traon, and G. Reverdin (2000), Global high-resolution mapping of ocean circulation from TOPEX/Poseidon and ERS-1 and 2, *J. Geophys. Res.*, *105*, 19,477–19,498, doi:10.1029/2000JC900063.

Feely, R., J. Bullister, and M. Roberts (1994), *Hydrographic, Chemical and Carbon Data Obtained During the R/V Discoverer Cruise in the Pacific Ocean During WOCE Section P18 (EXPOCODE 31DSCG94_1,2,3), (26 January-27 April, 1994)*, Carbon Dioxide Inf. Anal. Cent., Oak Ridge Natl. Lab., U.S. Dep. of Energy, Oak Ridge, Tenn., doi:10.3334/CDIAC/otg.31DSCG94_1_2_3. [Available at http://cdiac.ornl.gov/ftp/oceans/p18woce_noaa/.]

Fernández-Álamo, M. A., and J. Färber-Lorda (2006), Zooplankton and the oceanography of the eastern tropical Pacific: A review, *Prog. Oceanogr.*, *69*, 318–359.
Fiedler, P. C., and L. D. Talley (2006), Hydrography of the eastern tropical Pacific: A review, *Prog. Oceanogr.*, *69*, 143–180.
Fiedler, P. C., R. Mendelssohn, D. M. Palacios, and S. J. Bograd (2013), Pycnocline variations in the Eastern Tropical and North Pacific, 1958–2008, *J. Clim.*, *26*, 583–599, doi:10.1175/JCLI-D-11-00728.1.
Filonov, A., and I. Tereshchenko (2000), El Niño 1997–98 monitoring in mixed layer at the Pacific Ocean near Mexico's west coast, *Geophys. Res. Lett.*, *27*(5), 705–707.
Friederich, G. E., J. Ledesma, O. Ulloa, and F. P. Chavez (2008), Air-sea carbon dioxide fluxes in the coastal southeastern tropical Pacific, *Prog. Oceanogr.*, *79*, 156–166.
Friis, K., A. Körtzinger, and D. W. R. Wallace (2003), The salinity normalization of marine inorganic carbon chemistry data, *Geophys. Res. Lett.*, *30*(2), 1085, doi:10.1029/2002GL015898.
Cooperative Global Atmospheric Data Integration Project (2013), updated annually, Multi-laboratory compilation of synchronized and gap-filled atmospheric carbon dioxide records for the period 1979-2012 (obspack_co2_1_GLOBALVIEW-CO2_2013_v1.0.4_2013-12-23), Compiled by NOAA Global Monitoring Division: Boulder, Colo., doi:10.3334/OBSPACK/1002.
Godínez, V. M., E. Beier, M. F. Lavín, and J. A. Kurczyn (2010), Circulation at the entrance of the Gulf of California from satellite altimeter and hydrographic observations, *J. Geophys. Res.*, *115*, C04007, doi:10.1029/2009JC005705.
Hernández-Ayón, J. M., G. Gaxiola Castro, F. Chávez, T. Takahashi, D. Feely, C. Sabine, B. Hales y, and J. R. Lara Lara (2010), Variabilidad espacial y temporal del flujo de CO_2 océano-atmósfera. En: edited by G. Gaxiola-Castro and R. Durazo, "Dinámica del ecosistema pelágico frente a Baja California, 1997-2007. Diez años de investigaciones mexicanas de la Corriente de California," Secretaría de Medio Ambiente y Recursos Naturales, pp. 197–208.
Johnson, K. M., J. M. Sieburth, P. J. L. Williams, and L. Brandstrom (1987), Coulometric total carbon dioxide analysis for marine studies: Automation and calibration, *Mar. Chem.*, *21*, 117–133.
Kessler, W. S. (2006), The circulation of the eastern tropical Pacific: A review, *Prog. Oceanogr.*, *69*, 181–217.
Körtsinger, A., J. C. Duinker, and L. Mintrop (1997), Strong CO_2 emissions from the Arabian Sea during south-west monsoon, *Geophys. Res. Lett.*, *24*, 1763–1766.
Kurczyn, J. A., E. Beier, M. F. Lavín, and A. Chaigneau (2012), Mesoscale eddies in the northeastern Pacific tropical-subtropical transition zone: Statistical characterization from satellite altimetry, *J. Geophys. Res.*, *117*, C10021, doi:10.1029/2012JC007970.
Lavín, M. F., E. Beier, J. Gómez-Valdez, V. M. Godínez, and J. García (2006), On the summer poleward coastal current off SW México, *Geophys. Res. Lett.*, *33*, L02601, doi:10.1029/2005GL024686.
Lavín, M. F., R. Castro, E. Beier, V. M. Godínez, A. Amador, and P. Guest (2009), SST, thermohaline structure, and circulation in the southern Gulf of California in June 2004 during the North American monsoon experiment, *J. Geophys. Res.*, *114*, C02025, doi:10.1029/2008JC004896.
Le Traon, P. Y., Y. Faugère, F. Hernandez, J. Dorandeau, F. Mertz, and M. Ablain (2003), Can we merge GEOSAT Follow-On with TOPEX/Poseidon and ERS-2 for an improved description of the ocean circulation?, *J. Atmos. Oceanic Technol.*, *20*, 889–895, doi:10.1175/1520-0426(2003)020<0889:CWMGFW>2.0.CO2.
Lewis, E., and D. W. R. Wallace (1998), *Program Developed for CO_2 System Calculations, ORNL/CDIAC-105*, Carbon Dioxide Inf. Anal. Cent., Oak Ridge Natl. Lab., U.S. Dep. of Energy, Oak Ridge, Tenn.
León-Chávez, C. A., L. Sánchez-Velasco, E. Beier, M. F. Lavín, V. M. Godínez, and J. Färber-Lorda (2009), Larval fish assemblages and circulation in the Eastern Tropical Pacific in autumn and winter, *J. Plankton Res.*, *32*, 397–410, doi:10.1093/plankt/fbp138.
López-Sandoval, D. C., J. R. Lara-Lara, M. F. Lavín, S. Álvarez-Borrego, and G. Gaxiola-Castro (2009), Primary productivity in the Eastern Tropical Pacific off Cabo Corrientes, Mexico, *Cienc. Mar.*, *35*(2), 169–182.
Maske, H., R. Cajal-Medrano, A. Trasviña-Castro, A. Jiménez-Mercado, C. O. Almeda-Jauregui, G. Gaxiola-Castro, and J. Ochoa (2010), Inorganic carbon and biological oceanography above a shallow oxygen minimum in the entrance to the Gulf of California in the Mexican Pacific, *Limnol. Oceanogr. Methods*, *55*, 481–491.
Mehrbach, C., C. H. Culberson, J. E. Hawley, and R. M. Pytkowickz (1973), Measurement of the apparent dissociation constants of carbonic acid in seawater at atmospheric pressure, *Limnol. Oceanogr.*, *18*, 897–907.
Paulmier, A., D. Ruiz-Pino, V. Garçon, and L. Farías (2006), Maintaining of the Eastern South Pacific Oxygen Minimum Zone (OMZ) off Chile, *Geophys. Res. Lett.*, *33*, L20601, doi:10.1029/2006GL026801.
Paulmier, A., D. Ruíz-Pino, and V. Garçon (2008), The oxygen minimum zone (OMZ) off Chile as intense source of CO_2 and N_2O, *Cont. Shelf. Res.*, *28*, 2746–2756, doi:10.1016/j.csr.2008.09.012.
Paulmier, A., D. Ruíz-Pino, and V. Garçon (2011), CO_2 maximum in the oxygen minimum zone (OMZ), *Biogeosciences*, *8*, 239–252.
Roden, G. I. (1971), Aspects of the transition zone in the northeastern Pacific, *J. Geophys. Res.*, *76*(15), 3462–3475.
Sarmiento, J. L., and N. Gruber (2006), *Ocean Biogeochemical Dynamics*, Princeton Univ. Press, Princeton, N. J.
Simpson, J. H. (1981), The shelf-sea fronts: Implications of their existence and behavior, *Philos. Trans. R. Soc. London A*, *302*, 531–546.
Simpson, J. J., and A. Zirino (1980), Biological control of pH in the Peruvian coastal upwelling area, *Deep Sea Res., Part A*, *27*, 733 – 744.
Takahashi, T., J. Olafsson, J. G. Goddard, D. W. Chipman, and S. C. Sutherland (1993), Seasonal variation of CO_2 and nutrients in the high-latitude surface oceans: A comparative study, *Global Biogeochem. Cycles*, *7*, 843–878.
Takahashi, T., et al. (2002), Global sea-air CO_2 flux based on climatological surface ocean pCO2, and seasonal biological and temperature effect, *Deep Sea Res., Part II*, *49*, 1601–1622.
Takahashi, T., et al. (2009), Climatological mean and decadal change in surface ocean pCO_2, and net sea-air CO_2 flux over the global oceans, *Deep Sea Res., Part II*, *56*, 554–577.
Takahashi, T., S. C. Sutherland, and A. Kozyr (2013), *Global Ocean Surface Water Partial Pressure of CO_2 Database: Measurements Performed During 1957–2012 (Version 2012), ORNL/CDIAC-160, NDP-088(V2012)*, Carbon Dioxide Inf. Anal. Cent., Oak Ridge Natl. Lab., U.S. Dep. of Energy, Oak Ridge, Tenn., doi:10.3334/CDIAC/OTG.NDP088(V2012).
Wanninkhof, R. (1992), Relationship between wind speed and gas exchange over the ocean, *J. Geophys. Res.*, *97*, 7373–7382.
Weiss, R. F. (1970), The solubility of nitrogen, oxygen and argon in water and seawater, *Deep Sea Res., Part II*, *17*, 721–735.
Weiss, R. F. (1974), Carbon dioxide in water and seawater: The solubility of a non-ideal gas, *Mar. Chem.*, *2*, 203–215.
Zirino, A., and S. H. Lieberman (1985), *pH-Temperature Relationships in the Gulf of California in Mapping Strategies in Chemical Oceanography*, pp. 393–408, Am. Chem. Soc., Washington, D. C., doi:10.1021/ba-1985-0209.ch020.